Short communication

Preparation of Li_3BO_3–Li_2SO_4 glass–ceramic electrolytes for all-oxide lithium batteries

CrossMark

Masahiro Tatsumisago [a, *], Ryohei Takano [a], Kiyoharu Tadanaga [b], Akitoshi Hayashi [a]

[a] Department of Applied Chemistry, Graduate School of Engineering, Osaka Prefecture University, 1-1, Gakuen-cho, Naka-ku, Sakai, Osaka 599-8531, Japan
[b] Division of Materials Chemistry, Faculty of Engineering, Hokkaido University, Kita 13, Nishi 8, Kita-ku, Sapporo, Hokkaido 060-8628, Japan

H I G H L I G H T S

- Oxide Li_3BO_3–Li_2SO_4 electrolytes were prepared by mechanical milling.
- Conductivity of the $Li_{2.9}B_{0.9}S_{0.1}O_{3.1}$ glass–ceramic was 1.4×10^{-5} S cm^{-1} at 25 °C.
- A high temperature Li_3BO_3 phase was precipitated in the glass–ceramic electrolyte.
- A solid-state battery with the glass–ceramic was assembled by cold pressing.
- All-oxide solid-state $In/LiCoO_2$ batteries operated as a secondary battery at 25 °C.

A R T I C L E I N F O

A B S T R A C T

Newly designed oxide glass–ceramic electrolyte of $Li_{2.9}B_{0.9}S_{0.1}O_{3.1}$ with high Li$^+$ ion conductivity and low melting property was prepared by mechanical milling and subsequent heat treatment at 290 °C. This material showed 1.4×10^{-5} S cm^{-1} at room temperature and excellent deformation properties to obtain powder-compressed pellets with low interfacial resistance like in the case of sulfide solid electrolytes. The glass–ceramic exhibited favorable mechanical properties to form favorable solid–solid contacts in solid-state batteries by pressing without high temperature heat treatments. All-solid-state $In/LiCoO_2$ cells using these oxide glass–ceramic electrolytes operated as secondary batteries at room temperature.

© 2014 Elsevier B.V. All rights reserved.

1. Introduction

Safety and reliability are the most important points in next-generation battery systems that will be developed for our bright and clean-energy future society. It is believed that all-solid-state batteries using inorganic solid electrolytes are one of the ultimate goals of rechargeable energy sources for future vehicles and energy storage systems [1,2]. Single cation conduction and no solvation of carrier ions in inorganic solid electrolytes, which result in less side reactions and wide electrochemical windows, will provide us with an ideal battery system with a high level of safety and reliability. Another advantage of all-solid-state batteries is their possible use of active materials with high capacity such as metallic lithium and elemental sulfur, which are difficult to use in an organic liquid electrolyte cell.

Sulfide solid electrolytes of crystals [3,4], glasses [5] and glass–ceramics [6,7] are promising for all-solid-state batteries because of their high ionic conductivities around 10^{-2} S cm^{-1} at room temperature [4,7] comparable to organic liquid electrolytes. In the case of glass–ceramic electrolytes, the superionic high temperature crystalline phase like $Li_7P_3S_{11}$ [8], which could not be obtained by the usual solid state reaction, was precipitated by the heat treatment of the glass. Stabilization of superionic high temperature phase is one of the most effective techniques to obtain highly ionic conductors like in the case of stabilization of α-AgI in a glass matrix at room temperature [9]. Sulfide electrolytes have another merit of achieving good solid/solid contacts by only cold-press without high temperature sintering because of their excellent formability at ambient temperature [10]. One negative point of sulfide electrolytes is their instability under ambient atmosphere with moisture.

On the other hand, oxide-based solid electrolytes are very attractive for application in all-solid-state batteries because of their

high stability in regular air atmosphere without possibility of generating hydrogen sulfide from the electrolytes. In spite of such a big advantage of stability, oxide solid electrolytes are very difficult to use in all-solid-state batteries mainly because of their poor deformability at room temperature, which results in a huge interfacial resistance between electrolytes and electrodes [10]. High temperature sintering of oxide electrolytes sometimes causes chemical reactions between electrolytes and electrodes, which also generate large interfacial resistances.

In order to obtain excellent oxide solid electrolytes suitable for application in all-solid-state rechargeable batteries, "low melting property" is one of the most important features because of the following points: (1) Higher ion conductivities at room temperature are basically obtained in glassy materials with lower glass-transition temperatures. (2) Low melting materials, which exhibit lower cohesive energy, tend to show higher formability at room temperature. (3) Superionic high temperature phases can be obtained and stabilized at lower temperatures in glassy systems with lower glass-transition temperatures.

We discovered a series of Li^+ ion conducting glasses in lithium ortho-oxosalt pseudobinary systems such as $Li_4SiO_4–Li_3BO_3$ [11]. Since then, a variety of this type of mixed-anion or mixed-former glasses as oxide solid electrolytes have been developed by rapid melt quenching and mechanochemical techniques [12,13]. In these lithium ortho-oxosalt pseudobinary systems, the $Li_3BO_3–Li_2SO_4$ glassy system is very attractive with respect to its low melting properties and possibility of stabilization of superionic high temperature phases; such phases of Li_3BO_3 and Li_2SO_4 with high ionic conductivity have been reported [14,15]. So we have been focusing on the $Li_3BO_3–Li_2SO_4$ glassy materials to evaluate their possibility as an excellent oxide solid electrolyte for the application to all-solid-state battery systems. In our recent preliminary experiments, we have successfully prepared highly conductive $Li_3BO_3–Li_2SO_4$ glass-ceramics, which will be used for oxide-based all-solid-state batteries.

The present paper reports the preparation and characterization of the $Li_3BO_3–Li_2SO_4$ glasses and glass-ceramics and the application of these newly obtained materials to oxide-based all-solid-state lithium secondary batteries using conventional electrode active materials.

2. Experimental

Starting materials were $LiOH \cdot H_2O$ (>99%; Wako Chem.), H_3BO_3 (>99%; Wako Chem.) and $Li_2SO_4 \cdot H_2O$ (>99%; Aldrich Chem.). A mixture of $LiOH \cdot H_2O$ and H_3BO_3 were heated in an Al_2O_3 crucible at 500 °C for 1 h and then sintered at 600 °C for 2 h in air to obtain Li_3BO_3 crystal. $Li_2SO_4 \cdot H_2O$ was heated at 300 °C for 2 h under Ar flow to obtain anhydrous Li_2SO_4 crystal. The $Li_3BO_3–Li_2SO_4$ glasses were prepared by a mechanical milling technique (Fritsch Pulverisette 7). A mixture of the crystals of Li_3BO_3 and Li_2SO_4 was put into a 45 ml ZrO_2 pot with 160 ZrO_2 balls (5 mm in diameter) and milled at the rotating speed of 370 rpm with the milling period of 40–100 h. The Li_3BO_3 glass was prepared by the mechanical milling of Li_2O and B_2O_3 crystals for 40 h. All processes were conducted in a dry Ar atmosphere. Glass–ceramic samples were prepared by heating the glass samples.

Differential thermal analyses (DTA) were performed using a thermal analyzer (Thermo-plus 8120; Rigaku Corp.) to observe crystallization temperatures. The glass samples were heated at 10 °C min^{-1} under N_2 gas flow up to 900 °C. X-ray diffraction (XRD) measurements (CuKα) were conducted using a diffractometer (Ultima IV; Rigaku Corp.) to identify crystal phases of the glass-–ceramic samples. Ionic conductivities were measured for the pelletized samples pressed under 360 or 720 MPa with and without
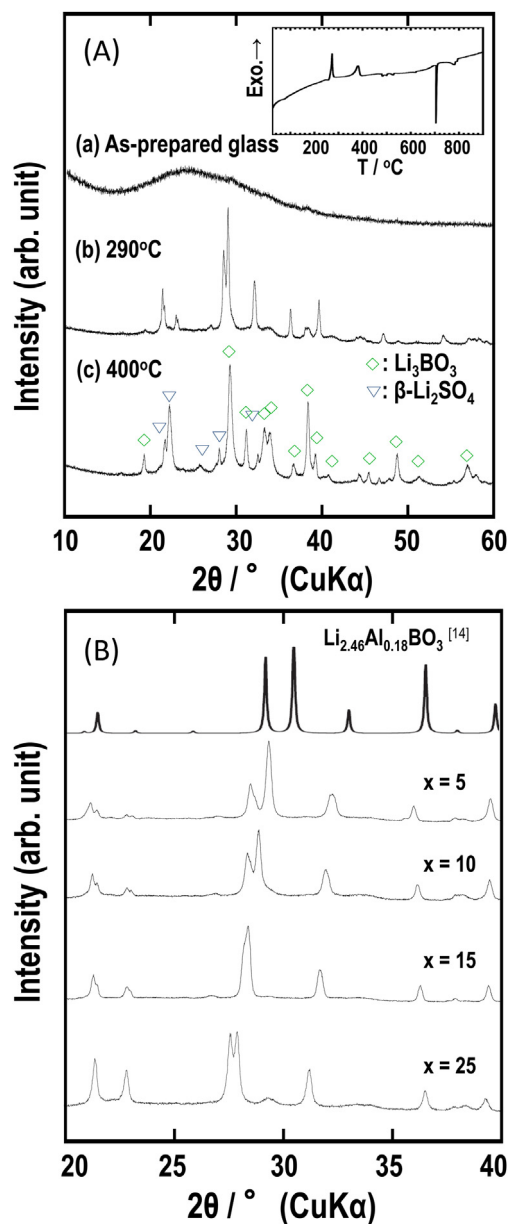

Fig. 1. (A) XRD patterns for the $Li_{2.9}B_{0.9}S_{0.1}O_{3.1}$ (90$Li_3BO_3 \cdot$ 10Li_2SO_4 in mol%) samples, as-prepared glass (a) and heat-treated ones at 290 °C (b) and 400 °C (c). The inset is a differential thermal analysis (DTA) curve for the glass. (B) XRD patterns for the crystallized $Li_3BO_3–Li_2SO_4$ glasses heat-treated at temperatures just beyond the first crystallization peak in DTA curve. The XRD pattern of $Li_{2.46}Al_{0.18}BO_3$ [14] is also shown in this figure for comparison.

subsequent heat treatment. The pellet diameter and thickness were 10 mm and about 1 mm, respectively. Gold electrode was deposited by vacuum evaporation on both faces of the pellets. Then stainless steel disks were attached to the pellets as current collectors. The prepared cell was sealed in a silica glass tube. Then AC impedance measurements were conducted under dry Ar gas flow using an impedance analyzer (SI-1260; Solartron). The frequency range and the applied voltage were, respectively, 0.1 Hz to 1 MHz and 50 mV. The AC impedance measurements were conducted at 25 °C for the glass samples. Then the pellets were heated to beyond the crystallization temperatures to obtain glass–ceramics. The impedances of glass–ceramic samples were measured after cooling the pellets to 25 °C. The apparent density of the powder-compressed pellets was calculated from the weight and volume of the pellets and the
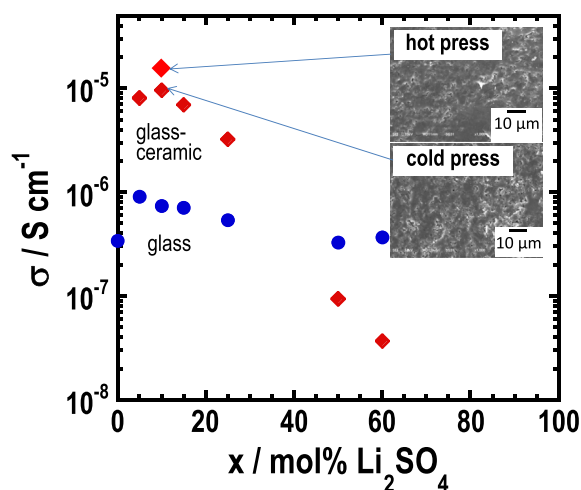
Fig. 2. Composition dependence of ionic conductivity at room temperature for mechanochemically prepared Li_3BO_3–Li_2SO_4 glasses and the corresponding glass–ceramics heat-treated at temperatures just beyond the first crystallization peak. The insets show the SEM photographs the powder-compressed pellet of $Li_{2.9}B_{0.9}S_{0.1}O_{3.1}$ prepared by cold-press at room temperature and hot-press at 255 °C.

apparent packing density was calculated by dividing the apparent density of the pellet by the theoretical density of the mixture calculated from the densities of component materials. The microstructure of a cross section of the electrolyte pellets was observed by SEM (JEOL, JSM-6610A). Cross sections of the battery samples were prepared by fracturing or by using an ion milling system that employs an Ar ion beam (E−3500, Hitachi High-Technologies).

An all-solid-state cell (In/$90Li_3BO_3 \cdot 10Li_2SO_4$ glass–ceramic solid electrolyte/$LiCoO_2$) was constructed to investigate its electrochemical performance as follows. $LiCoO_2$ particles without coatings (bare $LiCoO_2$) and with $LiNbO_3$ coatings (coated $LiCoO_2$ [16]) were used as an active material. The positive electrode was composed of the particles of $LiCoO_2$ (70 wt %) and $Li_{2.9}B_{0.9}S_{0.1}O_{3.1}$ ($90Li_3BO_3 \cdot 10Li_2SO_4$ in mol%) glass–ceramic (30 wt%). The $Li_{2.9}B_{0.9}S_{0.1}O_{3.1}$ glass–ceramic electrolyte was used as a separator.

Indium foil (Furuuchi Chem., 99.999%; 0.1 mm thickness) was used as a negative electrode. Stainless steel powders were used at the positive electrode side for securing electronic conduction and mechanical strength of the pellet. A three-layer pellet (10 mm in diameter) consisting of current collector, positive electrode and separator layers was prepared by pressing the powders of stainless steel, $LiCoO_2$ and $Li_{2.9}B_{0.9}S_{0.1}O_{3.1}$ glass under 360 MPa at room temperature (cold-press) or at 245 °C (hot-press) for 4 h. The pellets were heated at 290 °C to crystallize the $Li_{2.9}B_{0.9}S_{0.1}O_{3.1}$ glass. An indium film was coated on the negative electrode side by vacuum evaporation, an indium foil as a negative electrode was attached to the pellet and the pellet was sandwiched between two stainless steel rods as a current collector. The pellet was then heated at about 155 °C for 1 h. The all-solid-state cell was charged and discharged using a charge−discharge measuring device (BTS-2004; Nagano Co., Ltd.) at room temperature in a dry Ar atmosphere.

3. Results and discussion

Mechanical milling was carried out for $x = 0, 5, 10, 15, 25, 50, 60$ of $(100-x)Li_3BO_3 \cdot xLi_2SO_4$ (mol%) compositions. Glassy samples were obtained in all the compositions, in which XRD amorphous patterns were observed, by 40−100 h mechanical milling of the mixture of Li_3BO_3 and Li_2SO_4 crystals. Fig. 1(A) shows XRD patterns of the $90Li_3BO_3 \cdot 10Li_2SO_4$ samples, as-prepared glass (a) and heat-treated ones at 290 °C (b) and 400 °C (c). The as-prepared glass is showing a halo pattern typical of amorphous materials. DTA curve of the as-prepared glass is shown in the inset. This DTA curve suggests that the glass-transition temperature of this material is around 250 °C. In addition, two sharp exothermic peaks due to crystallization are observed at 260 and 360 °C. The heat treatment temperatures of 290 and 400 °C in Fig. 1 are just after these exothermic peaks. Although the diffraction peaks observed after the heat treatment at 400 °C are ascribed to stable phases of Li_3BO_3 and β-Li_2SO_4 crystals, the peaks observed after the heat treatment at 290 °C are not attributable to stable crystalline phases. The product obtained by the heat treatment at 290 °C is probably a metastable phase as in many cases of first recipitation from glassy materials [17]. Fig. 1(B) shows the XRD patterns for the crystallized
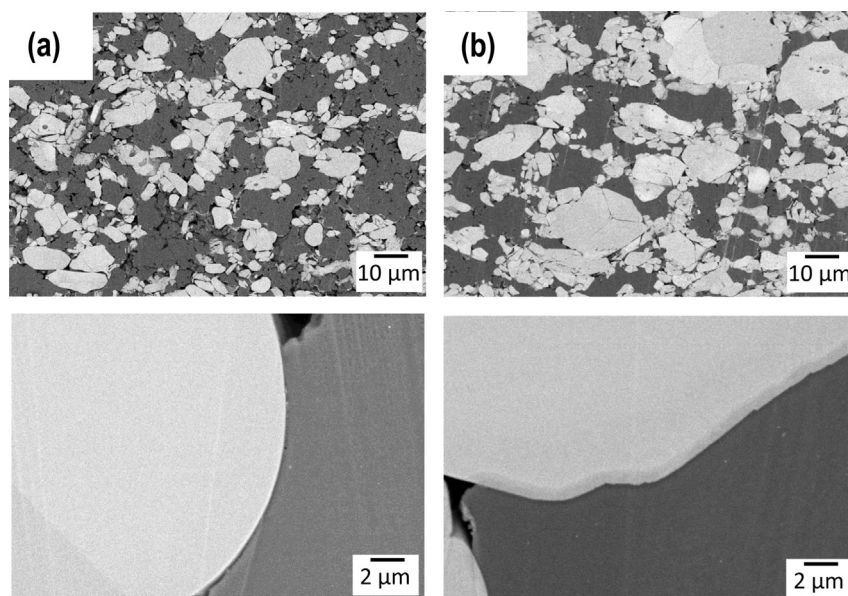

Fig. 3. The cross-sectional SEM image of the positive electrode layer composed of $LiCoO_2$ active material and $Li_{2.9}B_{0.9}S_{0.1}O_{3.1}$ glass electrolyte prepared by cold-press at room temperature (a) and hot-press at 255 °C (b).
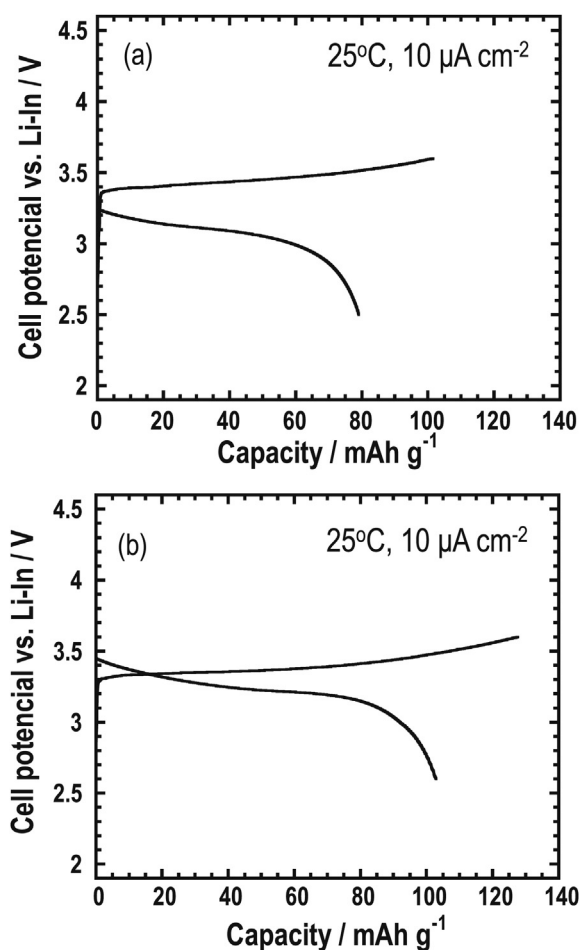
Fig. 4. The first charge−discharge curves of all-solid-state In/LiCoO$_2$ batteries using only Li$_{2.9}$B$_{0.9}$S$_{0.1}$O$_{3.1}$ glass−ceramic as a solid electrolyte prepared by cold-press (a) and hot-press at 245 °C (b) and subsequent heat treatment at 290 °C.

Li$_3$BO$_3$−Li$_2$SO$_4$ glasses heat-treated at temperatures just beyond the first crystallization peak, in which metastable phases might be precipitated. The high temperature phase of Li$_3$BO$_3$ was reported to stabilize with the addition of small amounts of aluminum ions [14]; the XRD pattern of Li$_{2.46}$Al$_{0.18}$BO$_3$, which possesses the crystal structure at high temperature phase of Li$_3$BO$_3$, is shown in this figure for comparison. It is apparent that the diffraction patterns of the crystallized Li$_3$BO$_3$−Li$_2$SO$_4$ are very similar to that of Li$_{2.46}$Al$_{0.18}$BO$_3$ and there are successive variations in the patterns with the changing Li$_2$SO$_4$ content. Since the diffraction peak shift is observed successively with the composition change, the precipitated metastable phases from the glasses are considered as solid solutions of high temperature phases of Li$_3$BO$_3$ and Li$_2$SO$_4$. It is necessary to make a further investigation on the detailed structure analyses using the diffraction data.

Fig. 2 shows the composition dependence of ionic conductivity at room temperature for mechanochemically prepared Li$_3$BO$_3$−Li$_2$SO$_4$ glasses and the corresponding samples heat-treated at temperatures just beyond the first crystallization peak. These data were obtained for the powder-compressed pellet samples in both cases. The conductivities of Li$_3$BO$_3$−Li$_2$SO$_4$ glasses ranges 10^{-7}–10^{-6} S cm^{-1} in the whole composition range. The increase of conductivity is observed with the addition of small amounts of Li$_2$SO$_4$. This is probably due to the so-called "mixed-former effect" and/or the improvement of packing density of the pellet, which also comes from the anion mixing of the glasses. In fact, the apparent

density of cold-pressed 90Li$_3$BO$_3$·10Li$_2$SO$_4$ glasses was 1.84 g cm^{-3}, which was much larger than that of Li$_3$BO$_3$ (1.53 g cm^{-3}). The crystallized samples, which can be called as glass-ceramics, exhibit much higher room temperature conductivities around 10^{-5} S cm^{-1} with the composition 90Li$_3$BO$_3$·10Li$_2$SO$_4$. This conductivity enhancement is attributable to the fact that the metastable crystalline phases analogous to the high temperature phase of Li$_3$BO$_3$ were precipitated in this glass−ceramic material. Since the glass powder shows an excellent deformation character, the powder-compressed pellet prepared by the cold press of glass at room temperature and then the heat treatment at 290 °C is quite dense as shown in the inset SEM photograph of Fig. 2. Grain boundaries are hardly visible in the cold-pressed sample. Cold-press of sulfide-based electrolytes decreases grain-boundaries and voids at the adjacent particles, and we term this densification "room-temperature pressure sintering" [10]. Similar behavior is probably observed in the present case. Our Raman spectroscopy study confirmed that the 90Li$_3$BO$_3$·10Li$_2$SO$_4$ electrolyte was composed of lithium ions (Li$^+$), orthoborate ions (BO$_3^{3-}$) and sulfate ions (SO$_4^{2-}$). These isolated ions are thought to diffuse at the particle boundaries on pressing at room temperature. The glass-transition temperature of 90Li$_3$BO$_3$·10Li$_2$SO$_4$ glass is around 250 °C, and thus the much denser glass−ceramic pellet can be obtained by hot-press at 255 °C and then heat treatment at 290 °C (Fig. 2 inset). This hot-pressed 90Li$_3$BO$_3$·10Li$_2$SO$_4$ glass−ceramic exhibits 1.4×10^{-5} S cm^{-1} at room temperature as shown in Fig. 2.

Fig. 3 shows the cross-sectional SEM images of the positive electrode composites, in which the particles of bare LiCoO$_2$ (70 wt %) and Li$_{2.9}$B$_{0.9}$S$_{0.1}$O$_{3.1}$ (90Li$_3$BO$_3$·10Li$_2$SO$_4$ in mol%) glass (30 wt%) were mixed and formed by cold-press at room temperature (a) and hot-press at 255 °C (b). Since the Li$_{2.9}$B$_{0.9}$S$_{0.1}$O$_{3.1}$ glass materials show an excellent deformation character as seen in the inset of Fig. 2, the interfaces between particles of LiCoO$_2$ and the glass materials are quite smooth in both cases of cold-press (a) and hot-press (b). Good contacts between them are achieved by pressing without high temperature heat treatments. The apparent packing densities of the cold-pressed and hot-pressed positive electrodes calculated from their observed apparent densities were respectively 70 and 78%, which is comparable to the values of those using sulfide glassy electrolytes [18].

Fig. 4 shows the first charge−discharge curves of all-solid-state In/LiCoO$_2$ batteries using only Li$_{2.9}$B$_{0.9}$S$_{0.1}$O$_{3.1}$ glass−ceramic as a solid electrolyte prepared by cold-press (a) and hot-press (b). In both cases coated-LiCoO$_2$ particles were used. The positive electrode parts in these batteries have the similar morphology to the powder-compressed pellets shown in Fig. 3 and the separator parts have the similar morphology to the insets of Fig. 2 for the cold-pressed and hot-pressed batteries. These batteries, in which the first discharge capacities are 78−102 mAh g^{-1} and the cell voltages are 3.2−3.4 V, operate as a secondary battery. It was found that all-oxide solid-state bulk-type rechargeable batteries prepared without high temperature sintering firstly worked like in the case of all-solid-state sulfide-based batteries. This is the first step to develop low temperature production of high performance all-solid-state oxide-based batteries.

4. Conclusions

We have developed oxide glass and glass−ceramic electrolytes in the system Li$_3$BO$_3$−Li$_2$SO$_4$. Crystallization of 90Li$_3$BO$_3$·10Li$_2$SO$_4$ glass increased conductivity by the precipitation of high temperature Li$_3$BO$_3$ phase. A high room temperature conductivity of 1.4×10^{-5} S cm^{-1} and an excellent deformation character were achieved in this oxide glass−ceramic electrolyte. Bulk-type all-solid-state rechargeable cells using 90Li$_3$BO$_3$·10Li$_2$SO$_4$

glass–ceramic were prepared by pressing without high temperature heat treatments. These all-oxide solid-state batteries operate as a secondary battery, which is the first step to develop low temperature production of all-solid-state oxide-based batteries.

References

[1] K. Takada, Acta Mater. 61 (2013) 759.
[2] M. Tatsumisago, M. Nagao, A. Hayashi, J. Asian Ceram. Soc. 1 (2013) 17.
[3] R. Kanno, A. Murayama, J. Electrochem. Soc. 148 (2001) A742.
[4] N. Kamaya, K. Homma, Y. Yamakawa, M. Hirayama, R. Kanno, M. Yonemura, T. Kamiyama, Y. Kato, S. Hama, K. Kawamoto, A. Matsui, Nat. Mater. 10 (2011) 682.
[5] M. Ribes, B. Barrau, J.L. Souquet, J. Non-Cryst. Solids 38 (1980) 271.
[6] F. Mizuno, A. Hayashi, K. Tadanaga, M. Tatsumisago, Adv. Mater. 17 (2005) 918.
[7] Y. Seino, T. Ota, K. Takada, A. Hayashi, M. Tatsumisago, Energy Environ. Sci. 7 (2014) 627.
[8] H. Yamane, M. Shigbata, Y. Shimane, T. Junke, Y. Seino, S. Adams, K. Minami, A. Hayashi, M. Tatsumisago, Solid State Ionics 178 (2007) 1163.
[9] M. Tatsumisago, Y. Shinkuma, T. Minami, Nature 335 (1991) 217;
M. Tatsumisago, T. Saito, T. Minami, Chem. Lett. (2001) 790.
[10] A. Sakuda, A. Hayashi, M. Tatsumisago, Sci. Rep. 3 (2013) 2261.
[11] M. Tatsumisago, N. Machida, T. Minami, J. Ceram. Soc. Jpn. 95 (1987) 59.
[12] M. Tatsumisago, H. Narita, T. Minami, M. Tanaka, J. Am. Ceram. Soc. 66 (1983) C210.
[13] A. Hayashi, D. Furusawa, Y. Takahashi, K. Minami, M. Tatsumisago, Phys. Chem. Glasses: Eur. J. Glass Sci. Technol. B 54 (2013) 109.
[14] M. He, H. Okudera, J. Fleig, A. Simon, X.L. Chen, J. Maier, J. Solid State Chem. 178 (2005) 680.
[15] E.A. Secco, J. Solid State Chem. 96 (1992) 366.
[16] N. Ohta, K. Takada, I. Sakaguchi, L. Zhang, R. Ma, K. Fukuda, M. Osada, T. Sasaki, Electrochem. Commun. 9 (2007) 1486.
[17] A. Hayashi, M. Tatsumisago, Electron. Mater. Lett. 8 (2012) 199.
[18] M. Tatsumisago, A. Hayashi, Int. J. Appl. Glass Sci. (2014), http://dx.doi.org/10.1111/ijag.12084 in press.